Proceedings World Geothermal Congress 2020
Reykjavik, Iceland, April 26 – May 2, 2020

Hydrochemistry of Produced Water from the Pohang EGS Project Site, Korea: Implications for Water-rock Reactions and Associated Changes to the State of Stress Accompanying Hydraulic Fracturing of Granite

Rob Westaway*, Neil M. Burnside and David Banks

James Watt School of Engineering, University of Glasgow, James Watt (South) Building, Glasgow G12 8QQ, UK

*robert.westaway@gla.ac.uk

Keywords: Pohang, Korea, EGS, granite, anthropogenic seismicity, hydrochemistry, geomechanics

ABSTRACT

During August 2017, ~1700 m^3 of water was injected into, and subsequent allowed to flowback from, the ~4 km deep PX-1 well, drilled into Permian granite at Pohang, Korea. Sampling of this produced water and its hydrochemical analysis, for major elements, trace elements, and stable isotopes, has provided an important dataset for the investigation of water-rock reactions in granite. As a first approximation, the variations in composition of this produced water are consequences of mixing of end-member compositions representing the injected surface water and in situ groundwater. The majority of the produced water was in situ groundwater, indicating that only a small proportion, estimated as only ~400 m^3, of the injected surface water was recovered; the rest remained in the subsurface. Superimposed on these variations are increases in concentrations of ionic species, which reflect chemical reactions between the injected surface water and the granite. These include silica from hydrolysis of quartz, sodium from hydrolysis of feldspar, and sulphate probably from hydrolysis of pyrite, this latter mineral forming deposits that line fractures within the Pohang granite. The M_W 5.5 Pohang earthquake occurred on 15 November 2017, three months after this injection experiment, in close proximity to the EGS site, initiating discussion regarding the possibility of a cause-and-effect connection. This oblique reverse-faulting earthquake occurred on the Namsong Fault, which passes above the injection point and transects the wellbore, its hypocentre being within a kilometre of the injection. We explore the possibility that injection at the EGS site might have caused this earthquake. Assuming that the injected surface water that was not recovered entered this fault, and given the ~160 °C ambient temperature, we calculate timescales for chemical re-equilibration of different ionic species. Re-equilibration of silica, for example, is thus estimated to require roughly three months, the time difference between the injection and the earthquake. We thus derive a quantitative model for this process, in which hydrochemical re-equilibration is envisaged as occurring by dissolution of asperities, where patches of fault are in mechanical contact, thus 'unclamping' the fault. This model leads to a new scaling law between injected volume and the maximum seismic moment, or magnitude, of resulting induced seismicity. This new scaling law is less conservative than existing theory, which assumes that pore space throughout a rock volume is flooded with injected fluid, because only the volume of the fault is flooded, the surrounding granite having extremely low porosity. It is thus shown that net injection of ~1000 m^3 of surface water can account for an induced earthquake comparable to that observed, provided that the seismogenic fault was already critically stressed. This analysis does not prove, of course, that the August 2017 injection experiment caused the M_W 5.5 Pohang earthquake; this earthquake might, for example, have been a consequence of the combined effect of all five injection experiments that took place at this site during 2016-2017 (three in well PX-2, including one in September 2017, and two in well PX-1), before the Korean authorities forced suspension of the EGS project. It nonetheless provides a salutary warning of a potential adverse consequence of injection of surface water into granite. A conceivable remedy, albeit at considerable cost, would be to inject water containing dissolved ionic species that match as closely as possible, or indeed exceed, the concentrations in the local groundwater.

1. INTRODUCTION

The Pohang EGS project is located in the southeast of Korea, ~6 km north of the centre of the industrial city of Pohang and ~3 km east of the town of Heunghae (Fig. 1(a)). Key details of this project will be summarized here; more details are provided elsewhere (e.g., Park et al., 2017; Lee et al., 2019; Westaway and Burnside, 2019). Two deep wells have been drilled, reaching ~4.3 km depth in Permian granite, one (PX-2) vertical and the other (PX-1) also initially drilled vertically, subsequently side-tracked to a WNW deviation by ~600 m (Figs 1(b),(c)), the bottom hole depths (below sea-level) being 4189 m for well PX-1 and 4314 m for well PX-2. Magnetotelluric exploration early in the project revealed a zone of high electrical conductivity, interpreted as a water-bearing fault, dipping steeply NW. However, subsequent investigations led to revision of the developers' conceptual model which, in its final form, envisaged utilization for fluid circulation of a WNW-ESE fracture, thus not incorporating the previously-identified NW-dipping fault into the project design. A significant loss of circulation of drilling fluid was noted at 3434 m depth during the initial (vertical) drilling of well PX-1, indicating that a permeable fault or fracture had been crossed. An even greater loss of circulation was reported, concentrated between depths of 3816 and 3840 m, during drilling of well PX-2, directly beneath a zone of fault gouge spanning 3790-3816 m (Fig. 2). These observations indicate that a major fault was transected. The latter loss of circulation (amounting to ~650 m^3) in November 2015, was followed by a 'burst' of microearthquakes lasting roughly a month, indicating that this major fault, or other faults hydraulically connected to it, were already critically stressed. However, this fault intersection was subsequently sealed by casing the wellbore. Injection experiments, to attempt to stimulate the geothermal reservoir, using hydraulic fracturing or 'hydroshearing' to improve its hydraulic properties, took place in well PX-1 in December 2016 and in August 2017, and in well PX-2 in February 2016, April 2017 and September 2017 (e.g., Kim et al., 2018); the overall volume injected into both wells has been ~12,000 m^3, with ~7000 m^3 of flowback (Hofmann et al., 2019).

The 'cloud' of aftershocks that followed the Pohang mainshock (Fig. 1(c)) reveals a NW-dipping fault plane in the same place (given the uncertainties in the studies) as the fault recognized in the preliminary exploration; to facilitate discussion, Westaway and Burnside (2019) designated this hitherto un-named structure as the Namsong Fault, named after a nearby village (Fig. 1(a)). Grigoli et al. (2018) and Kim et al. (2018) deduced that the Namsong Fault has a dip of 65-66° from seismological studies and modelling of surface deformation, as in Fig. 1(c). However, Lee et al. (2019) favour a much lower dip, of 43°. With this lower-angle dip, the Namsong Fault projects barely 100 m below the bottom of well PX-1 whereas with the alternative steeper dips it projects hundreds of metres deeper, as in Fig. 1(c). As is also shown in Fig. 1(c), the fault plane delineated by these aftershock locations projects across the wellbore at ~3800 m depth, consistent with the reported fault gouge and loss of circulation in well PX-2 (Fig. 2). The Pohang mainshock involved reverse slip with a component of right-lateral slip (Grigoli et al., 2018; Kim et al., 2018). The ~4 cm maximum coseismic uplift of the Earth's surface, revealed by satellite radar imaging, confirms the geometry of the fault (Grigoli et al., 2018). Logging tools inserted into well PX-2 in August 2018 could not reach below 3783 m depth (Lee et al., 2019), suggesting that this well had been sheared by the coseismic slip in November 2017 on the fault depicted in Fig. 2. The Namsong Fault, thus reactivated, has no mapped surface trace and was unrecognized before the November 2017 earthquake, except for the initial tentative interpretation of the magnetotelluric evidence, which did not inform the ultimate design of the EGS project.

The standard procedure (Davis and Frohlich, 1993) for assessing whether an earthquake is anthropogenic considers spatial proximity and temporal correlation with fluid injection, and geomechanical calculations indicating that the injection could have caused the seismogenic fault to slip, the latter typically relating shear and normal stresses and fluid pressure to the standard Coulomb failure criterion. For the Pohang mainshock, spatial proximity is obvious (Fig. 1(c)). The fluid pressure reached very high values during the first injection experiment in well PX-2 in February 2016, with maximum wellhead pressure 89 MPa causing bottom-hole pressure 132 MPa at 4368 m depth, exceeding the estimated minimum principal stress at depth (Park et al., 2017); had this pressure been transmitted directly to the Namsong Fault (i.e., had the fluid pressure acting on this fault risen to 132 MPa or any similar value) it would have slipped during this injection (Westaway and Burnside, 2019). Regarding any temporal association, full details of the subsequent injection experiments have not been reported by the developers; however, the published summaries (e.g., Kim et al., 2018) include injection in well PX-1 in August 2017 and in well PX-2 in September 2017, respectively three and two months before the mainshock. Although physical mechanisms are known that can cause seismicity delayed following fluid injection (e.g., Davies et al., 2013; Westaway, 2017), none has hitherto provided a satisfactory explanation for a delay as long as 2-3 months.

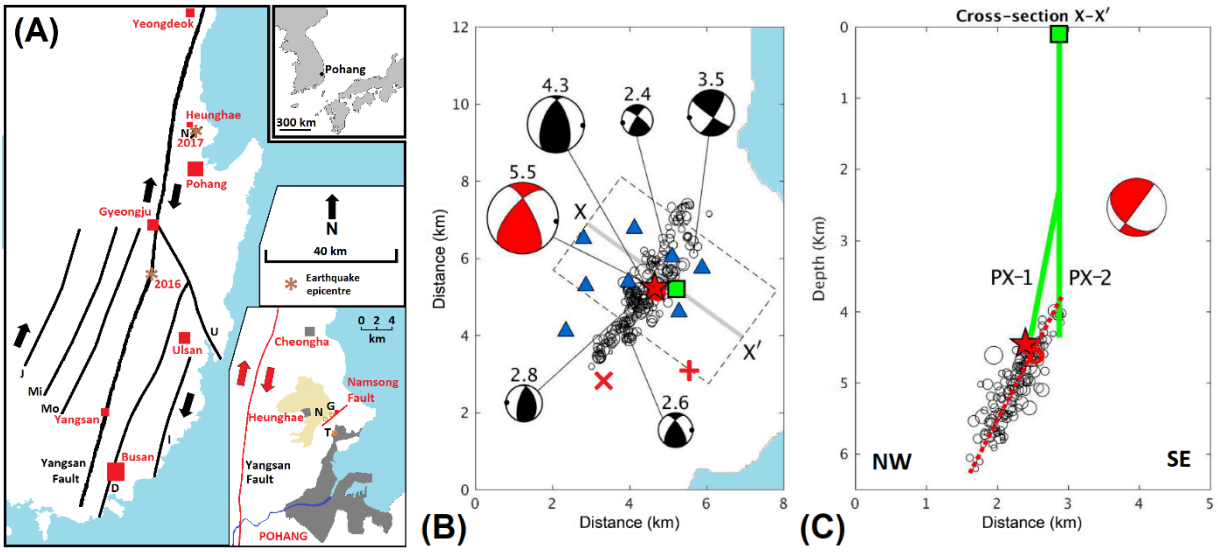

Figure 1: Location map for the city of Pohang in the SE part of the Korean peninsula (upper inset showing wider location, lower inset showing greater local detail), showing Late Cenozoic right-lateral faults, the Namsong Fault, and the epicentres of the 12 September 2016 and 15 November 2017 earthquakes (both of M_W ~5.5). The local inset shows the Namsong Fault (depicted schematically), the Heunghae alluvial plain (pale shading), the EGS project site (G), Namsong village (N), and the Pohang thermal spa resort that yielded hydrochemical data (T). (b) map, and (c) NW-SE cross-section along line illustrated in (b), showing schematically the two deep wells at the Pohang EGS site (solid green lines) and the interpreted plane of the Namsong Fault (dashed red line). Also showing locations of earthquakes at Pohang in November 2017: foreshocks (red circles); the 15 November mainshock (red star); and aftershocks (black circles), stations of the local seismograph network (blue triangles), the EGS site (green square), the thermal spa resort (red + symbol), and a borehole that yielded in situ stress measurements (red × symbol). Focal mechanisms of the mainshock and five principal aftershocks, each labelled by Mw, are drawn as standard lower (or back) focal hemisphere projections with compressional quadrants shaded. Modified from Figs 1 and 2 of Westaway and Burnside (2019), where other sources of information are documented; parts (b) and (c) are derived from Kim et al. (2018).

2. HYDROCHEMICAL DATA

To shed light on the processes occurring within the Pohang granite, we have investigated the hydrochemistry of samples of water produced from both the deep wells. As Hofmann et al. (2019) have discussed, the experimental protocol for the August 2017 stimulation of well PX-1 required flowback following the fluid injection. A systematic programme of sampling and analysis of this produced water, in addition to the surface water that was used for injection, was carried out, as Westaway and Burnside (2019) and Burnside et al. (in review) have described. Other water samples were collected from both deep Pohang wells at other times, enabling the composition of the groundwater in the Pohang granite to be identified. An initial conclusion from this work was that the groundwater has very different compositions in each of these wells, that in well PX-2 being a much more concentrated brine (Westaway and Burnside, 2019). This is consistent with Fig. 2, which shows that the Namsong Fault has a thick impermeable core, thus hydraulically isolating the rocks on either side, the open-hole section of well PX-1 being above this fault in its hanging-wall and that of well PX-2 being below the fault in its footwall (Fig. 1(c)).

Results of this analysis are summarized in Fig. 3. As an initial step in interpretation of these data, we note that the volume of the PX-1 wellbore was 74 m^3 (cased) and 11 m^3 (open-hole), a total of 85 m^3. This means that the last 74 m^3 of water injected, and therefore the first 74 m^3 produced, remained within the casing and thus had no opportunity to react with the granite. The initial samples of produced water to be collected evidently remained within the wellbore; the variability of their composition therefore probably reflects the variable composition of the injected surface water, which was abstracted from a nearby irrigation pond. The next feature evident is that the concentrations of dissolved species tend from initial values similar to those of the surface water to limiting values similar to those of the pre-exiting groundwater in this well. Westaway and Burnside (2019) envisaged that such variations can be explained to a first approximation as a consequence of mixing of surface water with groundwater, the proportion of the former decreasing progressively as flowback proceeded, departures from this mixing pattern being attributable to hydrochemical reactions within the granite. With the exception of magnesium (Mg^{2+}), all the species depicted in Fig. 3 are more concentrated in the groundwater than in the surface water. Now that more thorough analysis of the samples, including additional dissolved species, has been carried out (Burnside et al., in review), additional analysis is possible. The idea that the hydrochemistry of groundwater in the Pohang area is governed by reactions with the granite is well-established (e.g., Kim et al., 2001); the issue that we have begun to address is which of these reactions occur on timescales relevant to this EGS project, as a result of the hydrochemical system being taken out of equilibrium by the injection of surface water.

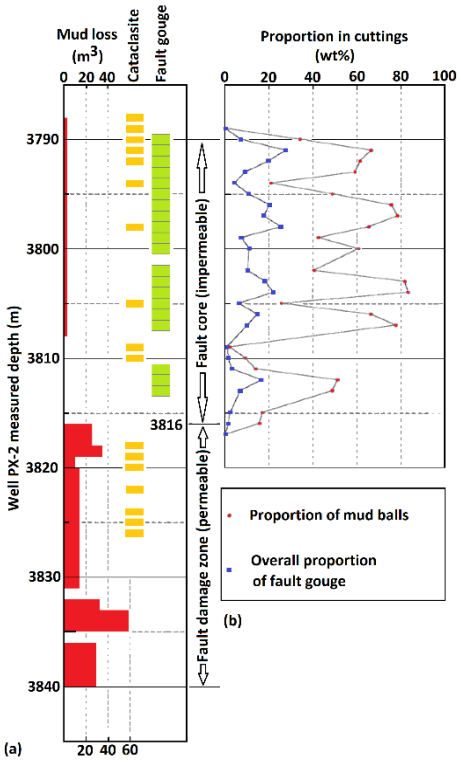

Figure 2: Enlargement of the intersection in Fig. 1(c) between well PX-2 and the Namsong Fault, showing (a) reports of fault gouge, cataclasite and loss of drilling mud, from drilling logs, and (b) proportions of fault gouge from subsequent laboratory analysis of cuttings. Modified from Fig. O-3(e) of Lee et al. (2019), based on Fig. 3 of Westaway and Burnside (2019). Many of the larger (centimetre-sized) cuttings from this depth range were 'mud balls' containing large proportions of fault gouge and cataclasite; Lee et al. (2019) provide further details. Interpretation of impermeable fault core and permeable fault damage zone is after Westaway and Burnside (2019).

We regard two of the dissolved species depicted in Fig. 3, boron (B) and chloride (Cl^-), as 'conservative', being affected by mixing but not to any significant extent by hydrochemical reactions. Although hydrochemical reactions involving these species have been recognized elsewhere (e.g., Munoz and Swenson, 1981; Bianchini et al., 2005), we have not envisaged them as significant within the Pohang granite, given its known geochemistry, over the timescales under consideration. As a check of this inference, we have modelled the variations in concentration of these species after Sauty (1980) (Fig. 4). This technique, which has previously been used to investigate other processes (e.g., mixing between groundwater and surface water in mines; Younger, 2000), assumes one-dimensional flow consisting of a combination of advection (i.e., bulk flow towards the well bottom) and dispersion (i.e., irregularities in flow patterns caused by tortuosity of flow paths, in this case through networks of fractures in the Pohang granite that are likely to be quite complex). Although this technique almost certainly provides only a crude approximation to the complexity of the flow at depth, it enables prediction of the variation in concentration over time of each dissolved species using only four model parameters: the Péclet number, Pe, a dimensionless measure of the 'vigour' of the flow, the transit time t_C for purely advective flow to the well bottom from the point where the groundwater enters the volume previously flooded by injected surface water, and the initial and final concentrations of the species at the well bottom. The fact that both species modelled are consistent with the same values of Pe and t_C (Fig. 4) suggests that this approach is on the right track, although the lesser mismatch between observed and predicted concentrations for Cl^- than for B suggests that the latter species might in fact be affected to a limited extent by hydrochemical reaction. The different patterns of variation in the concentrations of the other species (Fig. 3) can thus be inferred to result from hydrochemical reactions, their likely cause being dissolution or hydrolysis of minerals in the Pohang granite by the injected surface water.

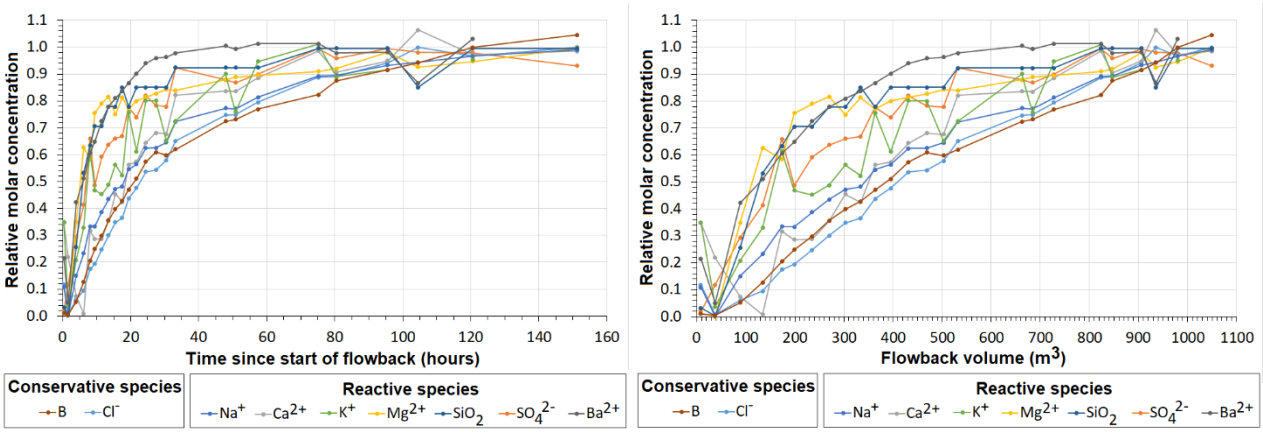

Figure 3: Molar compositions of key dissolved species in water produced from Pohang well PX-1, sampled in August 2017, normalized relative to initial values of zero and to values of one after 151 hours (left) or 1049 m^3 of flowback (right), plotted as functions of time (left) and produced water volume (right). Some of the species classified here as 'reactive' were evidently much more so than others, Ba^{2+} being the most reactive; conversely, the species listed as 'conservative' might participate in hydrochemical reactions to a limited extent (Fig. 4), so the distinction between these classifications is gradational. The abrupt change in composition after ~105 hours of flowback was caused by the cutting and removal of the inner well casing to install a submersible pump, which resulted in mixing of water that had previously occupied the casing annulus with the produced water. Data from Westaway and Burnside (2019) and Burnside et al. (in review).

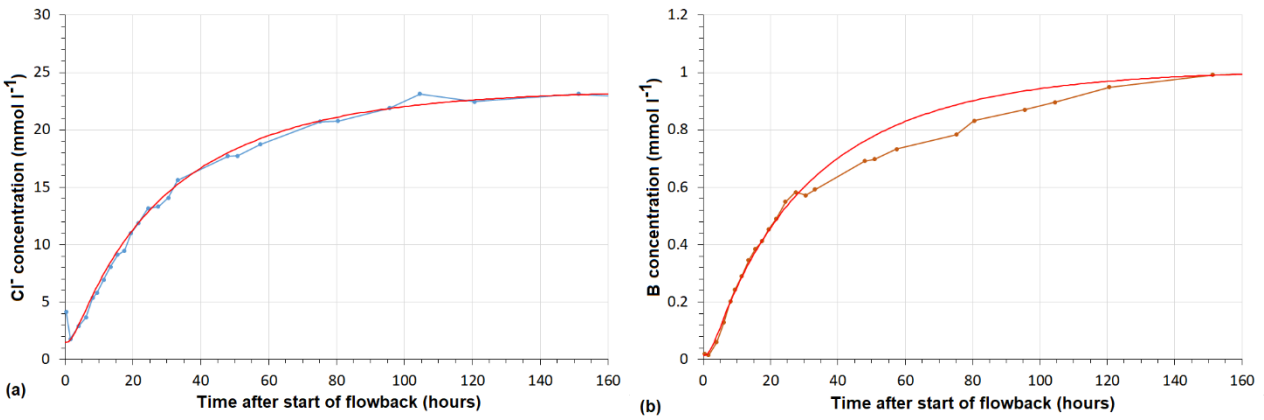

Figure 4: Molar compositions of 'conservative' dissolved species, modelled using equation (14) of Sauty (1980, using data from Westaway and Burnside (2019) and Burnside et al. (in review). For both species, Pe=1 and t_C=12 hours. (a) For chloride, assuming initial and final concentrations of 1.5 and 23.5 mmol l^{-1}. (b) For boron, assuming initial and final concentrations of 0.015 and 1.01 mmol l^{-1}.

The Pohang granite (*sensu lato*; granodiorite *sensu stricto*) consists of quartz, potassic feldspar, plagioclase, and biotite (Lee et al., 2014). Potential hydrolysis reactions thus include the dissolution of quartz (e.g., Rimstidt and Barnes, 1980):

$$SiO_2\ (s) + 2H_2O\ (l) \rightarrow H_4SiO_4\ (aq) \quad (1)$$

Hydrolysis of potassic feldspar (orthoclase) would yield the secondary clay mineral kaolinite as a solid residue, releasing potassium into solution as well as silicon in the form of silicic acid:

$$2KAlSi_3O_8\ (s) + 9H_2O\ (l) + 2H^+\ (aq) \rightarrow Al_2Si_2O_5(OH)_4\ (s) + 4H_4SiO_4\ (aq) + 2K+\ (aq) \quad (2)$$

Hydrolysis of plagioclase can be represented by the end-member reactions for albite:

$$2NaAlSi_3O_8\ (s) + 11H_2O\ (l) + 2CO_2\ (aq) \rightarrow Al_2Si_2O_5(OH)_4\ (s) + 4H_4SiO_4\ (aq) + 2HCO_3^-\ (aq) + 2Na^+\ (aq) \quad (3)$$

and for anorthite:

$$CaAl_2Si_2O_8\ (s) + 3H_2O\ (l) + 2CO_2\ (aq) \rightarrow Al_2Si_2O_5(OH)_4\ (s) + Ca^{2+}\ (aq) + 2HCO_3^-\ (aq) \quad (4)$$

(e.g., Kim et al., 2001); in both cases the solid reaction product depicted is again kaolinite. Equations (1), (2), and (3) simplify more complex behaviour, with silicon released as a mixture of silicic acid (H_4SiO_4) and pH-dependent complex silicate ions. A more complex set of equations, for intermediate composition of plagioclase, is provided by Banks and Frengstad, 2006). Alternatively, hydrolysis of plagioclase might produce the hydrous clay mineral smectite (montmorillonite) (e.g., Kato and Hirono, 2016):

$$2NaCaAl_3Si_5O_{16}\ (s) + (3n\text{-}4)H_2O\ (l) + 6H+\ (aq) + 2Si(OH)_4\ (aq) \rightarrow 3Al_2Si_4O_{10}(OH)_2.n(H_2O)\ (s) + 2Ca^{2+}\ (aq) + 2Na^+\ (aq) \quad (5)$$

this reaction being illustrated for the intermediate composition, labradorite. Under hydrothermal conditions, saturation of calcium in solution might result in dolomitization (e.g., Machel and Mountjoy, 1986):

$$Ca^{2+}\ (aq) + Mg^{2+}\ (aq) + 4HCO_3^-\ (aq) \rightarrow CaMg(CO_3)_2\ (s) + 2H_2O\ (l) + 2CO_2\ (l) \quad (6)$$

Excess potassium in solution might also be produced (along with silicon, again illustrated as silicic acid) by hydrolysis of biotite to the secondary minerals chlorite and boehmite (cf. Howard and Fisk, 1988; Bray et al., 2014):

$$2K(Mg,Fe)_3AlSi_3O_{10}(OH)_2\ (s) + 8H_2O\ (l) + H^+\ (aq) \rightarrow (Mg,Fe)_3AlSi_3O_{10}(OH)_2\ .\ (Mg,Fe)_3(OH)_6\ (s) + AlO(OH)\ (s) + 3H_4SiO_4\ (aq) + 2K^+\ (aq) \quad (7)$$

(for which charge is balanced, as the formula depicted for chlorite includes an Al^{3+} ion occupying a Si^{4+} site in the crystal lattice). About 1% of the Pohang granite by weight is iron (Lee et al., 2014); in outcrop of nearby granites, fractures are filled with pyrite (Westaway and Burnside, 2019). Hydrolysis of pyrite by oxygenated water will release iron and sulphate ions into solution, thus:

$$2FeS_2\ (s) + 7O_2\ (aq) + 2H_2O\ (l) \rightarrow 2Fe^{2+}\ (aq) + 4SO_4^{2-}\ (aq) + 4H^+\ (aq) \quad (8)$$

(e.g., Gzyl and Banks, 2007). A final reaction that might occur in granite is release into solution of barium, illustrated for barite:

$$BaSO_4\ (s) \rightarrow Ba^{2+}\ (aq) + SO_4^{2-}\ (aq) \quad (9)$$

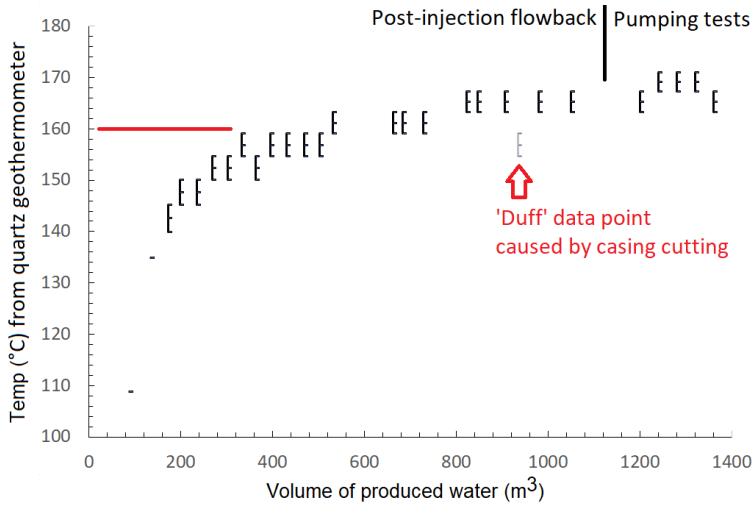

Figure 5: Temperature estimates by applying the Fournier (1977) quartz geothermometer to the dissolved silica in the produced water from well PX-1. Error bars reflect uncertainties in the experimental results, which were only reported to two significant figures: 160 mg SiO_2 l^{-1} during the latter stages of the post-injection flowback and up to 170 mg l^{-1} during the subsequent pumping tests. Data from Westaway and Burnside (2019) and Burnside et al. (in review).

The barium content of the Pohang granite has not been determined, but this element is often present in granites, for example as a trace constituent of potassic feldspar or in gangue minerals. The kinetics of barite dissolution have recently been investigated by Zhen-Wu et al. (2016); this process is sensitive to temperature and pressure so will be enhanced at downhole conditions. Concentration variations of Ba^{2+} under the conditions anticipated in the subsurface at Pohang can thus be anticipated to be particularly significant, providing a natural explanation for why the observed variations for this species show the greatest departure from a mixing pattern (Fig. 3).

This hydrochemical dataset also facilitates estimation of bottom hole temperature (BHT) from geothermometry. The Pohang EGS project was designed assuming a nominal bottom-hole temperature (BHT) of 180 °C, for a nominal 5 km depth, but measurements of the undisturbed BHT in wells PX-1 and PX 2 were not made by the developers. Nonetheless, a 103 °C temperature has been reported at 2250 m depth, just above the top of the Pohang granite at 2356 m (Yoon et al., 2015). The surface heat flow is 94 mW m^{-2} in a nearby borehole (Kim and Lee, 2007); given the 28 °C km^{-1} geothermal gradient in the granite (Kim and Lee, 2007) a temperature of ~160 °C can be estimated at ~4.3 km depth (i.e., 103 °C + (~4.3 – ~2.4 km) × 28 °C km^{-1} = ~160 °C). For comparison, Fig. 5 shows temperature estimates by applying the Fournier (1977) quartz geothermometer to the dissolved silica concentrations in the produced water from well PX-1. The temperature estimated after >800 m^3 of flowback, 165±2 °C, is in good agreement.

3. IMPLICATIONS FOR GEOMECHANICS

One potential candidate mechanism, poro-elastic diffusion of stress, has been proposed as the cause of 'natural' seismicity with delays of months following climatic triggering (e.g., Costain, 2017). Many case studies of seismicity associated with fluid injection or extraction have also been explained as poro-elastic effects (e.g., Segall, 1989; Segall et al., 1994; Chang and Segall, 2016; Chang and Yoon, 2018; Chang et al., 2018). Poro-elastic modelling of the flow rate / pressure dataset for the August 2017 stimulation of well PX-1 has been reported (e.g., Hofmann et al., 2019). However, this work is subject to significant limitations, first, because its analysis is two-dimensional (2-D), assuming cylindrical symmetry, with the injected fluid assumed to flow radially outward and not upward or downward. Second, it assumes that the flow is governed by matrix permeability and not fracture permeability, let alone permeability created by the development of new fractures as the injection proceeds. Such 2-D modelling has no way of incorporating any interaction between the injected fluid and the Namsong Fault; three-dimensional modelling is evidently desirable, but is beyond the scope of the present study. Nonetheless, hypocentral locations of the microearthquakes that accompanied this injection experiment indicate downward propagation below the ~4.2 km deep PX-1 injection point to a depth of ~4.4 km (Hofmann et al., 2019), the deepest adjoining the projection of the Namsong Fault below the injection point, especially if the dip of the fault is as low as 43° (cf. Fig. 1(c)). The lack of any deeper propagation suggests that the injected fluid may have interacted with this fault.

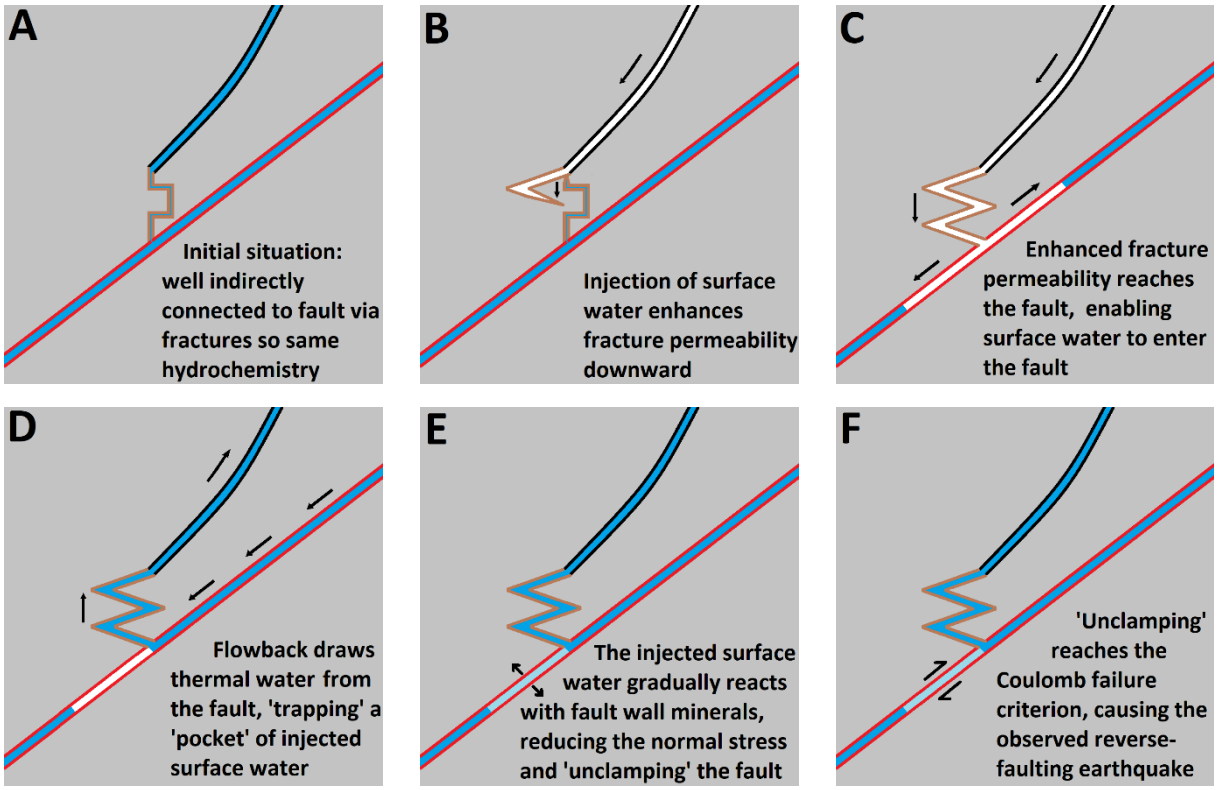

Figure 6: Conceptual model linking injection into well PX-1 to the 15 November 2017 earthquake. Panels depict NW-SE cross-sections across the Namsong Fault (cf. Fig. 1(c)), not to scale. The 'zig-zag' pattern of fracturing reflects the analysis indicating a preferred orientation, given the local stress field (with the minimum principal stress vertical; Lee et al., 2019; Westaway and Burnside, 2019), at 30° dip towards S69°E or N69°W, or towards N83°E or S83°W, depending on choice of model stress field. Using standard theory, the largest earthquake in August 2017 (M_W 1.9; Hofmann et al., 2019) would correspond to shearing of a fracture with dimensions no greater than ~50 m, indicating the probable upper bound to the individual 'zig-zag' fracture segments.

Poro-elasticity has also been proposed as the cause of the 15 November 2017 Pohang earthquake by Lee et al. (2019), their modelling treating the Pohang granite as a material of uniform (0.01 $m^2 s^{-1}$) hydraulic diffusivity, with a lower diffusivity for the Namsong Fault core and a higher diffusivity for the adjoining damage zone (cf. Fig. 2), thus – again – not explicitly incorporating the anticipated fractured nature of these fault rocks. This modelling did not investigate injection into well PX-1, but determined that the injection experiments in well PX-2 increased the fluid pressure on the Namsong Fault by ~0.1 MPa in April 2017 and by ~0.08 MPa by 15 November 2017, the latter change being regarded by these authors as the cause of the M_W 5.5 earthquake. However, realistic calculations of poro-elastic stress changes for a fractured material as complex as the Pohang Granite, as a consequence of fluid injection under a state of triaxial stress, would be extremely difficult, and are beyond the scope of the present study. Nonetheless, the fact that the above-mentioned calculations predict a smaller poro-elastic pressure increase at the Namsong Fault in November 2017 compared with at times beforehand means that the Lee et al. (2019) analysis does not in fact account for the timing of the 15 November 2017 earthquake. In addition, considerations of proximity between the two wells and the Namsong Fault indicate the potential importance of injection into well PX-1: the top of the open-hole section of well PX-2 is ~400 m below the Namsong Fault, whereas if this fault dips at only 43° (as Lee et al., 2019, deduced) it passes barely 100 m below the bottom of well PX-1, the aforementioned limited downward propagation of the seismicity accompanying this injection (Hofmann et al., 2019) thus suggesting that the injected fluid, and the fracture network it created, may have reached this fault. Such considerations raise the possibility that significant causal factors of the 15 November 2017 Pohang earthquake have been overlooked in the work reported so far, including the official report to the Korean government, by Lee et al. (2019), which was supposed to have been definitive.

Guided in part by the above considerations, we investigate another potential candidate mechanism for seismicity, the effect of injected surface water, reacting with the granite adjoining the fault, on the local state of stress. Such an effect can be inferred from studies of the alteration history of granite intrusions, which reveal precipitation of quartz within faults or fractures at temperatures of ~150 °C (e.g., Psyrillos et al., 2001), thus demonstrating interaction between solid and dissolved phases under such conditions. Such interaction is shown to be able to account for seismicity with delays of the order of months or years. Our analysis will focus on the August 2017 stimulation of well PX-1 as this is the best-documented hydrochemically of the Pohang injection experiments. However, this does not mean that we regard this injection as the sole cause of the M_W 5.5 earthquake; multiple injection experiments, plus the aforementioned release of drilling fluid, might well have contributed to hydrochemical 'corrosion' of the Namsong Fault, but the information available on these activities is incomplete. Furthermore, we cannot prove that injected surface water entered the Namsong Fault; no attempt has been made to sample the water in this fault, as would be necessary to validate our hypothesis. We note, nonetheless, that a future plan for re-habilitating the Pohang EGS site might involve utilizing circulation along the Namsong Fault. This could be achieved by perforating the casing of well PX-2 at the point where it crosses this fault and utilizing the existing hydraulic connection between well PX-1 and the fault (shown hypothetically in Fig. 6), or deepening well PX-1 to intersect the fault if no connection already exists. Such adaptations, and associated pumping tests, would provide the ability to sample the water within the Namsong Fault, allowing our hypothesis to be tested.

The hydrochemical dataset presented in Figs 3 and 4 indicates that well PX-1 is hydraulically connected to the groundwater within the granite. Moreover, although the volume of water produced from well PX-1 roughly equalled that injected in August 2017, because much of the produced water was 'natural' groundwater, it follows that much of the injected surface water (we estimate ~1400 m^3, or ~80%) remained within the granite. Figure 6 illustrates a conceptual model that might thus account for the 15 November earthquake. It assumes that the August 2017 injection into well PX-1 indeed enhanced fracture permeability downward, releasing surface water into the Namsong Fault. Subsequent flowback drew water from this fault: initially, injected surface water; subsequently, a mixture of surface water and groundwater; and, ultimately, groundwater, thus leaving a 'pocket' of surface water 'trapped' within the fault.

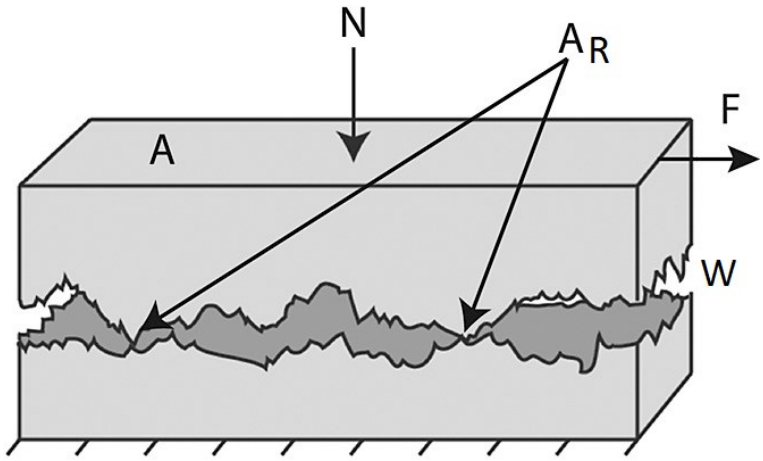

Figure 7: Conceptual model for a fault, modified after Mitchell et al. (2012). The fault is regarded as a fluid-filled volume of area A and typical width W, its surfaces – with fractal distributions of irregularities – being in contact at asperities of area A_R, with A_R<<A. N and F are the normal and shear forces acting across the fault, associated with the normal and shear stresses σ_N and τ.

Much work has been carried out on interactions between fluids within faults and earthquake processes (e.g., Yasuhara et al., 2005; Miller, 2013). A fault can thus be regarded as consisting of 'patches' in frictional contact, 'asperities', which provide frictional strength, separated by volumes occupied by fluid (as in Fig. 7). This fluid is usually at its equilibrium concentration; pressure solution resulting from the normal stress across a fault thus dissolves the tips of asperities, which are in contact, causing re-precipitation around their edges, widening the area in contact and strengthening the fault (Yasuhara et al., 2005). However, if the fluid is not in chemical equilibrium, as in Fig. 6(d)(e), dissolution at asperities will not be accompanied by re-precipitation elsewhere. Dissolution of a thin layer at any asperity will create space to enable the fault wall-rocks to decompress toward the fault, reducing the compressive normal stress and 'unclamping' the fault.

Our data (Fig. 3) provide strong evidence of dissolution, or hydrolysis, of quartz and other minerals in the Pohang granite on the timescale of flowback in August 2017. This inference is supported by simple calculations for the conditions at depth, including the 160 °C temperature, using the known rate constants for the various reactions (e.g., Rimstidt and Barnes, 1980; Gudbrandsson et al., 2014). Timescales for re-equilibration of silica as a function of temperature, in fractures of a given width, are shown in Fig. 8. Chemical re-equilibration of water within a fault thus provides a mechanism for post-injection anthropogenic seismicity, with a time-delay governed by the dissolution rate. Provided this process is governed by the kinetics of hydrolysis of quartz, Fig. 8 indicates that at 160 °C a three-month duration of hydrochemical and stress re-equilibration, and thus a three-month delay of post-injection seismicity, is feasible for a fault of typical width W=0.6 mm.

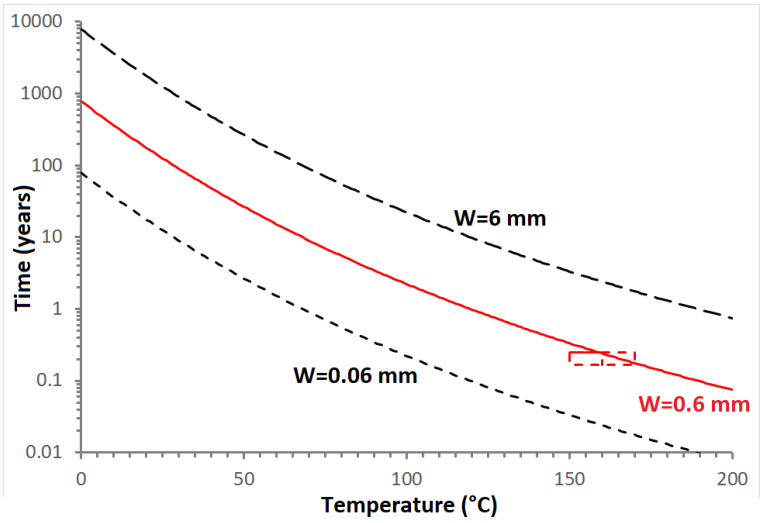

Figure 8: Timescales for equilibration of concentration of dissolved silica in fractures of width W (where W=0.06, 0.6, and 6 mm), after Rimstidt and Barnes (1980). Calculations assume silica concentrations of zero, initially, increasing to 99.3% of the equilibrium value, thus depicting five times the 'time constant' for the dissolution. Box represents a 160±10 °C temperature and a 2-3 month timescale, consistent with the bottom-hole temperature and post-injection time-delay observed at Pohang in 2017.

The magnitude M_W and seismic moment M_O of the largest earthquake that might thus be caused, after a volume V of surface water becomes 'trapped' within a fault (cf. Fig. 6(d)), can also be estimated. We adopt a conceptual model of a fault as illustrated in Fig. 7. The model fault is thus assumed permeable, with typical width W, and filled by fluid, the bounding rocks being impermeable. If the fault thus occupied has a square cross-section of side length L, then $V=W\times L^2$. If this area of fault slips, then from standard theory $M_O=\mu\times u\times L^2$, and the stress drop $\Delta\sigma=\mu\times u/L$, μ being the shear modulus of the adjoining rocks and u the spatial average coseismic slip. Combining these equations gives

$$M_O = \Delta\sigma\times(V/W)^{3/2} . \quad (10)$$

M_W can be calculated from M_O using the standard equation

$$\log_{10}(M_O/\text{N m}) = 9.05 + 1.5\times M_W \quad (11)$$

Taking V=1400 m^3 for the August 2017 injection, W=0.6 mm (Fig. 8), and $\Delta\sigma$=10 MPa (an upper bound; e.g., Ide and Beroza, 2001; Shaw, 2009), one obtains $M_O=4\times10^{16}$ N m and M_W=5.0, in reasonable agreement with the observed M_W=5.5. Taking V=2800 m^3, to allow for the possibility that an equal volume of surface water remained in the subsurface after the December 2016-January 2017 injection into well PX-1, but keeping the other parameter values the same gives $M_O=1\times10^{17}$ N m and M_W=5.3. Calculation assuming V=80% of the overall injected ~12,000 m^3 (e.g., Hofmann et al., 2019), or ~10,000 m^3, gives $M_O=7\times10^{17}$ N m and M_W=5.9.

For comparison, the existing theory by McGarr (2014) predicts

$$M_O = \mu \times V , \quad (12)$$

(with V now denoting the net volume injected) thus giving (in granite with μ=20 GPa) $M_O=4\times10^{13}$ N m and M_W=3.0 for injected volume V=1756 m^3, or $M_O=2\times10^{14}$ N m and M_W=3.6 for V=12,000 m^3 (or even lower values of M_O and M_W if one uses net injected volumes at Pohang, taking into account volumes of water subsequently produced). However, the derivation of this theory (McGarr, 2014) assumes that the injected water floods pore-space in the rock volume surrounding a fault rather than being localized within the fault; this assumption is inappropriate for injection into granite that has essentially zero porosity and permeability except within faults and fractures.

The rocks bounding the model fault in Fig. 7 are assumed to be held in frictional contact at asperities, which are assumed to follow a fractal size distribution; this means that they occupy area A_R that is proportional to the effective normal stress σ_N' (e.g., Archard, 1957; Mitchell et al., 2012) and much less than the fault area A, such that

$$A_R = k\,\sigma_N'\,A\,. \qquad (13)$$

Dissolution of these fault wall rocks, of density ρ_R, in response to chemical disequilibrium within this fluid, is assumed to be localized at these asperities (as a result of pressure solution; cf. Yasuhara et al., 2005), and to remove a thickness δW of rock from each as the fluid re-equilibrates. The mass of rock that dissolves is thus $\rho_R \times A_R \times \delta W$. This can be equated to the mass of material entering solution which will be $C \times A \times W$ if its concentration in the volume $A \times W$ increases from zero to C; one thus obtains

$$\frac{\delta W}{W} = \frac{C}{\rho_R\,k\,\sigma_N'}\,. \qquad (14)$$

As the asperities dissolve, the fault wall rocks will decompress toward the fault, moving inward on either side by distance δW/2, thus reducing the effective normal stress on the fault by $\delta\sigma_N$' where

$$\delta\sigma_N' = \frac{E\,\delta W}{2\,D}\,, \qquad (15)$$

D being the width (perpendicular to the fault) of the adjoining blocks and E their Young's modulus. Thus:

$$\delta\sigma_N' = \frac{E\,C\,W}{2\,D\,\rho_R\,k\,\sigma_N'}\,. \qquad (16)$$

To apply this analysis to Pohang, we take E=50 GPa (nominal value for granite), k σ_N' = ~0.03 (from Mitchell et al., 2012), from a numerical simulation of a fault with fractal roughness, for σ_N' ~135 MPa, this value being estimated by Westaway and Burnside, 2019), ρ_R=2650 kg m^{-3} for quartz, C ~200 mg l^{-1} for dissolution of quartz under the conditions at Pohang (Westaway and Burnside, 2019, calculated 186 mg l^{-1} for dissolved silica using PhreeqcI, before this species was analysed; the measurements indicate ~160-170 mg l^{-1}), W=0.6 mm (from the present analysis of the time delay for the seismicity; Fig. 8), and D ~0.5 m, from the fracture spacing in nearby granite outcrop (Westaway and Burnside, 2019), obtaining ~80 kPa for $\delta\sigma_N$'. If the Namsong Fault were already very close to the Coulomb condition for slip stability, as has been inferred (e.g., Lee et al., 2019; Westaway and Burnside, 2019), a small change in σ_N' such as this might cause for slip instability. Regardless of the choice of stress field model and slip sense, the relatively small magnitude of this change to the state of stress means that this fault must have already been very close to the condition for slip for this mechanism to explain the seismicity. Nonetheless, from equation (16), the predicted value of $\delta\sigma_N$' is proportional to W. Thus, for example, if the chemical disequilibrium within the Namsong Fault was caused by the first stimulation of well PX-2, starting in January 2016, the delay of ~1.8 years indicates W ~5 mm, giving $\delta\sigma_N$' ~0.6 MPa. If caused by the aforementioned loss of circulation into the fault during the drilling of well PX-2 in November 2015 (e.g., Lee et al., 2019), the ~2 year delay indicates similar values for W and $\delta\sigma_N$'. Furthermore, if the disequilibrium was caused by the loss of circulation into the fault during the drilling of well PX-1, with its original vertical orientation, in the Autumn of 2013 (Yoon et al., 2015), the ~4 year delay indicates W ~10 mm, predicting $\delta\sigma_N$' ~1.2 MPa. These calculations omit any cooling effect of the injected water, on the basis that any such effect will be minor, with duration much less than these timescales (Westaway and Burnside, 2019). Nonetheless, this mechanism can only account for small changes in the state of stress on a fault, by $\leq$~0.1 MPa for the analysis relating to the August 2017 injection into well PX-1, indeed implying that the Namsong fault must already have been very close to the condition for slip. Given the inter-relationships between W, temperature and time-delay (Fig. 8), an anthropogenic earthquake with M_W>5.0, with a shorter delay, might be predicted in rocks at 160 °C for V=1400 m^3 for a fault with W<0.6 mm, although it requires the fault to already be even closer to the slip condition. Conversely, a longer delay might result for a fault with larger W, enabling a greater change in the stress state to the slip condition, although from equation (10) the largest earthquake feasible after a longer delay, for a given injected volume, would be smaller; furthermore, injection into a wider fault might in principle cause significant cooling, slowing the hydrochemical reactions and prolonging the time delay (cf. Fig. 8).

The conceptual model of a fault in Fig. 7 also bears upon the manner in which frictional behaviour of faults is incorporated into descriptions of the physics of seismicity. As already noted, analyses of the Pohang earthquake (e.g., those by Lee et al., 2019, and Westaway and Burnside, 2019) have used the standard Coulomb frictional slip criterion. Other workers (after Ruina, 1983) have taken to analyzing seismicity using the so-called 'rate-and-state friction' (RSF) approach, in which the coefficient of friction of a fault is assumed to vary as a function of its slip rate and slip history. The idea of RSF frictional laws originated in laboratory experiments, but the parameters required to quantify such laws cannot be readily 'upscaled' to real faults, and are often fitted in an 'ad hoc' manner in individual studies, which casts doubt on the validity of the approach. Workers (e.g., van den Ende et al., 2018) have recently attempted to reconcile, or integrate, the RSF approach with the microphysical behaviour of faults. Essential to such efforts is the recognition of the role of pressure solution within faults affecting the local state of stress, as in Fig. 8. There is thus clear

synergy between our analysis and this work; the Pohang EGS project might indeed be regarded as an unintentional experiment to demonstrate the role of fault microphysics and associated hydrochemistry in earthquake occurrence. Deliberate experiments to provide confirmation might also be considered, although preferably not at any site near a large city where large earthquakes are unexpected and no particular thought has been given to earthquake insurance or earthquake-resistant design of buildings.

The present analysis should be seen as an initial step at analyzing a complex dataset that bears upon an issue of major importance. So far we have only quantified the effect of dissolution of quartz, whereas the hydrochemistry of the produced water suggests that the fluid injection into the Pohang granite has caused hydrolysis of multiple minerals – certainly quartz, plagioclase and biotite, possibly also potassic feldspar, probably also minerals forming fault and fracture infills such as pyrite and barite, plus probably also other minerals reflected in trace constituents of the produced water that have not yet been investigated. Fluid injection will also cause poro-elastic effects on the state of stress, as others (e.g., Lee et al., 2019) have discussed for Pohang, but our work suggests that over the timescales and under the conditions of interest these effects will be small compared with those of 'hydrochemical corrosion'. Furthermore, any poroelastic effects will ultimately dissipate, whereas 'hydrochemical corrosion' will have permanent effects. The injection experiments at Pohang might thus be regarded as unintentionally causing chemical stimulation through this mechanism, rather than, or in addition to, the intended hydraulic stimulation. Buijze et al. (2019) have recently published a worldwide inventory of seismicity associated with EGS projects, noting that this has been largely associated with projects involving injection into granite. The occurrence of 'hydrochemical corrosion' may well be the key factor, not hitherto considered, that has caused this difference between injection into granite and injection into other lithologies. Re-analysis of these instances, including the Landau, Germany and Basel, Switzerland, case-studies noted by Westaway and Burnside (2019), is therefore timely, as would be re-analysis of other case-studies involving injection into fractured metamorphic basement, of composition and physical state that can be expected to be similar to the Pohang granodiorite, such as the famous sequence of earthquakes at Denver, Colorado, in the 1960s, caused by injection of waste water (e.g., Healy et al., 1968). As Westaway and Burnside (2019) have noted, this effect might be mitigated in future EGS projects by injecting groundwater (or maybe 'synthetic' groundwater with composition that mimics the local 'natural' groundwater) rather than surface water, although this would have cost implications. Chemical or radioactive tracers might be injected in future EGS projects to trace the movement of the injected water in the subsurface; although this would be a new development in geothermics, tracer use has been standard in the oil industry and in hydrology for decades. Tracer use at Pohang would have immediately settled multiple issues that we have discussed. The possibility of 'hydrochemical corrosion' also places an obligation on EGS developers to identify any significant faults near their sites and to determine whether these faults are critically stressed; at Pohang, as noted above, the Namsong Fault was tentatively identified then disregarded during development, whereas the developers only undertook cursory studies of the state of stress, whose results (reported, e.g., by Park et al., 2017) have been shown to be incorrect and superseded by more recent analyses (e.g., those by Lee et al., 2019, and Westaway and Burnside, 2019). The idea that geomechanical models might one day form part of legal cases, as part of claims for compensation for losses caused by anthropogenic earthquakes, was foreseen some time ago (e.g., Westaway, 2006). Responsibility for the 15 November 2017 Pohang earthquake is now clear, but as the developer is already bankrupt the question of how the people affected will be compensated remains open.

4. CONCLUSIONS

The November 2017 M_W 5.5 Pohang earthquake is one of the largest and most damaging seismic events to have occurred in the Korean peninsula over the last century. Given its close proximity to the Pohang EGS site, and the resulting possibility that this earthquake was anthropogenic, we have investigated the possibility of a cause and effect connection, concentrating on the effect - hitherto not considered – of 'hydrochemical corrosion', whereby injection of surface water causes dissolution or hydrolysis of minerals within granite and thereby alters the state of stress. We have thus analysed the variation in composition of produced water from Pohang well PX-1 following the injection experiment in August 2017. As a first approximation, this variation can be explained as a consequence of mixing of the injected surface water with pre-existing groundwater, the effect being illustrated for chloride and boron in Fig. 4. Much of the injected surface water is thus inferred to have remained in the subsurface. Superimposed on these patterns are other variations, which we infer to result from reactions between the injected surface water and minerals within the Pohang granite. Dissolved species thus affected include sodium, calcium, potassium, magnesium, silica, sulphate, and barium (Fig. 3). We infer that the same hydrochemical reactions continued in the injected surface water that remained in the subsurface. Assuming this water was injected into the seismogenic Namsong Fault, as schematically illustrated in Fig. 6, we derive theory that can predict the magnitude and seismic moment of the largest feasible resulting earthquake, and the associated time delay, as a function of the conditions in, and properties of the fault. We thus show that hydrochemical changes occurring while modest volumes of surface water, injected into granite, re-equilibrates chemically with its subsurface environment, can account for changes to the state of stress potentially of the order of megapascals, and earthquakes as large as that at Pohang, after time delays as long as months or years, provided the seismogenic fault was already critically stressed, or very close to the condition for slip. This candidate causal mechanism counters the potential argument that the time delay and small injected volume militate against an anthropogenic cause of the Pohang earthquake. Our analysis thus places bounds on combinations of physical and chemical properties of rocks, injected volume, and potential post-injection time-delays for significant anthropogenic seismicity during future EGS projects in granite.

ACKNOWLEDGEMENTS

We are grateful for funding from the European Commission Horizon 2020 Research and Innovation Programme under grant agreement 691728 for project DESTRESS (DEmonstration of soft Stimulation TREatmentS of geothermal reservoirS). NMB is also funded by a University of Glasgow Lord Kelvin/Adam Smith Research Fellowship. We thank many DESTRESS co-workers, especially Günter Zimmermann and Hannes Hofmann, for helpful discussions.

REFERENCES

Archard, J.F.: Elastic deformation and the laws of friction. *Proceedings of the Royal Society of London, Series A, Mathematical and Physical Sciences*, **243**, (1957), 190–205.

Banks, B., and Frengstad, B.: Evolution of groundwater chemical composition by plagioclase hydrolysis in Norwegian anorthosites. *Geochimica et Cosmochimica Acta*, **70**, (2006), 1337–1355.

Bianchini, G., Pennisi, M., Cioni, R., Muti, A., Cerbai, N., Kloppmann, W.: Hydrochemistry of the high-boron groundwaters of the Cornia aquifer (Tuscany, Italy). *Geothermics*, **34**, (2005), 297-319.

Bray, A.W., Benning, L.G, Bonneville, S. and Oelkers, E.H.: Biotite surface chemistry as a function of aqueous fluid composition. *Geochimica et Cosmochimica Acta*, **128**, (2014), 58–70.

Buijze, L., van Bijsterveldt, L., Cremer, H., Paap, B., Veldkamp, H., Wassing, B., van Wees, J.-D., ter Heege, J.: Review of worldwide geothermal projects: mechanisms and occurrence of induced seismicity. Report TNO 2019 R100043, (2019), 257 pp. TNO, Utrecht, the Netherlands. http://publications.tno.nl/publication/34634288/pWlZ4Q/TNO-2019-R10043.pdf

Burnside, N.M., Westaway, R., Banks, D., Lee, J., Zimmermann, G., Hofmann, H., and Boyce, A., under review. Changes in chemistry of flowback fluid from a deep geothermal borehole in granodiorite, following hydraulic stimulation: Pohang, Korea. *Applied Geochemistry*, under review.

Chang, K.W. and Segall, P.: Injection-induced seismicity on basement faults including poroelastic stressing. *Journal of Geophysical Research: Solid Earth*, **121**, (2016), 2708-2726.

Chang, K.W. and Yoon, H.: 3-D modeling of induced seismicity along multiple faults: Magnitude, rate, and location in a poroelasticity system. *Journal of Geophysical Research: Solid Earth*, **123**, (2018), 9866-9883.

Chang, K.W., Yoon, H. and Martinez, M.J.: Seismicity rate surge on faults after shut-in: Poroelastic response to fluid injection. *Bulletin of the Seismological Society of America*, **108**, (2018), 1889-1904.

Costain, J.K.: Groundwater recharge as the trigger of naturally occurring intraplate earthquakes. In: Landgraf, A., Kübler, S., Hintersberger, E. and Stein, S. (eds), Seismicity, Fault Rupture and Earthquake Hazards in Slowly Deforming Regions. *Geological Society, London, Special Publication* **432**, (2017), 91–118.

Davies, R., Foulger, G., Bindley, A. and Styles, P.: Induced seismicity and hydraulic fracturing for the recovery of hydrocarbons. *Marine and Petroleum Geology*, **45**, (2013), 171-185.

Davis, S.D. and Frohlich, C.: Did (or will) fluid injection cause earthquakes? - Criteria for a rational assessment. *Seismological Research Letters*, **64** (3-4), (1993), 207-224.

Fournier, R.O.: Chemical geothermometers and mixing models for geothermal systems. *Geothermics*, **5**, (1977), 41-50.

Grigoli, F., Cesca, S., Rinaldi, A.P., Manconi, A., López-Comino, J.A., Clinton, J.F., Westaway, R., Cauzzi, C., Dahm, T. and Wiemer, S.: The November 2017 M_w 5.5 Pohang earthquake: A possible case of induced seismicity in South Korea. *Science*, **360**, (2018), 1003-1006.

Gudbrandsson, S., Wolff-Boenisch, D., Gislason, S.R. and Oelkers, E.H.: Experimental determination of plagioclase dissolution rates as a function of its composition and pH at 22 °C. *Geochimica et Cosmochimica Acta*, **139**, (2014), 154–172.

Gzyl, G., Banks, D.; Verification of the "first flush" phenomenon in mine water from coal mines in the Upper Silesian Coal Basin, Poland. *Journal of Contaminant Hydrology*, **92**, (2007), 66-86.

Healy, J.H., Rubey, W.W., Griggs, D.T., and Raleigh, C.B.: The Denver earthquakes. *Science*, **61**, (1968), 1301–1310.

Hofmann, H., Zimmermann, G., Farkas, M., Huenges, E., Zang, A., Leonhardt, M., Kwiatek, G., Martinez-Garzon, P., Bohnhoff, M., Min, K.-B., Fokker, P., Westaway, R., Bethmann, F., Meier, P., Yoon, K.S., Choi, J.W., Lee, T.J., Kim, K.Y.: First field application of cyclic soft stimulation at the Pohang Enhanced Geothermal System site in Korea. *Geophysical Journal International*, **217**, (2019), 926–949.

Howard, K.J. and Fisk, M.R.: Hydrothermal alumina-rich clays and boehmite on the Gorda Ridge. *Geochimica et Cosmochimica Acta*, **52**, (1988), 2269-2279.

Ide, S. and Beroza, G.C.: Does apparent stress vary with earthquake size? *Geophysical Research Letters*, **28**, (2001), 3349–3352.

Kato, N. and Hirono, T.: Heterogeneity in friction strength of an active fault by incorporation of fragments of the surrounding host rock. *Earth, Planets and Space*, **68**, 134, (2016), doi: 10.1186/s40623 016 0512 3.

Kim, C.S., Bae, D.S., Koh, Y.K., Kim, K.S., and Kim, G.Y.: Groundwater evolution of the granite area, Korea. In: Proceedings of International symposium on technologies for the management of radioactive waste from nuclear power plants and back end nuclear fuel cycle activities; Taejon (Republic of Korea); 30 August - 3 September 1999; Report IAEA-CSP--6/C, (2001), 10 pp. https://www-pub.iaea.org/MTCD/publications/PDF/csp_006c/PDF-Files/paper-66.pdf

Kim, H.C. and Lee, Y.: Heat flow in the Republic of Korea. *Journal of Geophysical Research*, **112**, B05413, (2007), doi: 10.1029/2006JB004266.

Kim, K.-H., Ree, J.-H., Kim, Y., Kim, S., Kang, S.Y., and Seo, W.: Assessing whether the 2017 M_w 5.4 Pohang earthquake in South Korea was an induced event. *Science*, **360**, (2018), 1007-1009.

Lee, K.-K., Yeo, I.-W., Lee, J.-Y., Kang, T.-S., Rhie, J., Sheen, D.-H., Chang, C., Son, M., Cho, I.-K., Oh, S., Pyun, S., Kim, S., Ge, S., Ellsworth, W.L., Giardini, D., Townend, J., Shimamoto, T.: Summary report of the Korean Government Commission on

relations between the 2017 Pohang earthquake and the EGS project. Geological Society of Korea and Korean Government Commission on the Cause of the Pohang Earthquake, Seoul, Republic of Korea, (2019), 205 pp. http://www.gskorea.or.kr/custom/27/data/Summary_Report_on_Pohang_Earthquake_March_20_2019.pdf

Lee, T.-H., Yi, K., Cheong, C.-S., Jeong, Y.-J., Kim, N., and Kim, M.-J.: SHRIMP U-Pb zircon geochronology and geochemistry of drill cores from the Pohang Basin. *Journal of the Petrological Society of Korea*, **23** (3), (2014), 167-185.

Machel, H.-G., and Mountjoy, E.W.: Chemistry and environments of dolomitization —a reappraisal. *Earth-Science Reviews*, **23**, (1986), 175–222.

Malmström, M., and Banwart, S.: Biotite dissolution at 25°C: The pH dependence of dissolution rate and stoichiometry. *Geochimica et Cosmochimica Acta*, **61**, (1997), 2779–2799.

McGarr, A.: Maximum magnitude earthquakes induced by fluid injection. *Journal of Geophysical Research, Solid Earth*, **119**, (2014), 1008–1019.

Miller, S.A.: The role of fluids in tectonic and earthquake processes. *Advances in Geophysics*, **54**, (2013), 1-46.

Mitchell, E.K., Fialko, Y. and Brown, K.M.: Temperature dependence of frictional healing of Westerly granite: experimental observations and numerical simulations. *Geochemistry, Geophysics, Geosystems*, **14**, (2012), 567–582.

Munoz, J.L. and Swenson, A.: Chloride-hydroxyl exchange in biotite and estimation of relative HCl/HF activities in hydrothermal fluids. *Economic Geology*, **76**, (1981), 2212-2221.

Park, S., Xie, L., Kim, K.-I., Kwon, S., Min, K.-B., Choi, J., Yoon, W.-S. and Song, Y.: First hydraulic stimulation in fractured geothermal reservoir in Pohang PX-2 well. *Procedia Engineering*, **191**, (2017), 829–837.

Psyrillos, A., Manning, D.A.C. and Burley, S.D.: The nature and significance of illite associated with quartz-hematite hydrothermal veins in the St. Austell pluton, Cornwall, England. *Clay Minerals*, **36**, (2001), 585–597.

Rimstidt, J.D. and Barnes, H.L.: The kinetics of silica-water reactions. *Geochimica et Cosmochimica Acta,* **44**, (1980), 1683-1699.

Ruina, A.: Slip instability and state variable friction laws. *Journal of Geophysical Research*, **88**, (1983), 10,359–10,370.

Sauty, J.-P.: An analysis of hydrodispersive transfer in aquifers. *Water Resources Research*, **16**, (1980), 145–158.

Segall, P.: Earthquakes triggered by fluid extraction. *Geology*, **17**, (1989), 942-946.

Segall, P., Grasso, J.-R. and Mossop, A.: Poroelastic stressing and induced seismicity near the Lacq gas field, southwestern France. *Journal of Geophysical Research*, **99**, (1994), 15423-15438.

Shaw, B.E.: Constant stress drop from small to great earthquakes in magnitude-area scaling. *Bulletin of the Seismological Society of America*, **99**, (2009), 871–875.

van den Ende, M.P.A., Chen, J., Ampuero, J.-P. and Niemeijer, A.R.: A comparison between rate-and-state friction and microphysical models, based on numerical simulations of fault slip. *Tectonophysics*, **733**, (2018), 273–295.

Westaway, R.: Investigation of coupling between surface processes and induced flow in the lower continental crust as a cause of intraplate seismicity. *Earth Surface Processes and Landforms*, **31**, (2006), 1480-1509.

Westaway, R.: Integrating induced seismicity with rock mechanics: a conceptual model for the 2011 Preese Hall fracture development and induced seismicity. In: Rutter, E.H., Mecklenburgh, J. and Taylor, K.G. (eds), Geomechanical and Petrophysical Properties of Mudrocks. *Geological Society, London, Special Publication* **454**, (2017), pp. 327-359.

Westaway, R., and Burnside, N.M., 2019. Fault "corrosion" by fluid injection: a potential cause of the November 2017 Mw 5.5 Korean earthquake. *Geofluids*, 1280721, (2019), 24 pp.

Yasuhara, H., Marone, C. and Elsworth, D.: Fault zone restrengthening and frictional healing: The role of pressure solution. *Journal of Geophysical Research*, **110**, B06310, (2005), doi:10.1029/2004JB003327.

Yoon, K.-S., Jeon, J.-S., Hong, H.-K., Kim, H.-G., Hakan, A., Park, J.-H. and Yoon, W.-S.: Deep drilling experience for Pohang enhanced geothermal project in Korea. Proceedings, World Geothermal Congress 2015, Melbourne, Australia, 19-25 April 2015.

Younger, P.L.: Predicting temporal changes in total iron concentrations in groundwaters flowing from abandoned deep mines: a first approximation. *Journal of Contaminant Hydrology*, **44**, (2000), 47–69.

Zhen-Wu, B.Y., Dideriksen, K., Olsson, J., Raahauge, P.J., Stipp, S.L.S., Oelkers, E.H.: Experimental determination of barite dissolution and precipitation rates as a function of temperature and aqueous fluid composition. *Geochimica et Cosmochimica Acta*, **194**, (2016), 193-210.